One-Dimensional Modulational Instability in a Crossed-Field Gap

Peggy J. Christenson and Y. Y. Lau

Department of Nuclear Engineering and Radiological Sciences, University of Michigan, Ann Arbor, Michigan 48109-2104

(Received 27 December 1995; revised manuscript received 18 March 1996)

Cycloidal electron flows in a gap with crossed electric and magnetic fields are found to be violently unstable when a small ac voltage is imposed across the gap. This instability is electrostatic and one dimensional. It occurs over a wide band of frequencies and is insensitive to the precise level of the injected current density. The physical origin of this instability is the formation of a virtual cathode right in front of the cathode. An analytic theory is presented which accurately predicts the onset of the instability in the low-frequency limit. [S0031-9007(96)00076-2]

PACS numbers: 52.25.Wz, 52.35.Ra, 52.65.Cc, 84.47.+w

Electrons flow in crossed electric and magnetic fields in many devices such as magnetron, crossed-field amplifier, magnetically insulated diode, and single-species particle trap experiment. As a result, there exists vast literature on the stability of such electron flows. With a few exceptions, most of the theories consider only equilibria in which all electrons flow at the local $\mathbf{E} \times \mathbf{B}$ velocity. Cycloidal motions in the equilibrium state are ignored altogether. The dominant instability is the diocotron instability, whose existence requires perturbation electric fields to vary in two directions [1].

In this paper, we report a new instability in cycloidal flows in a crossed-field gap. This instability is one dimensional, and its excitation requires only a small ac voltage imposed across the gap. It occurs over a wide range of frequencies, possibly from $1/10$ to a few times the electron cyclotron frequency. Its excitation is insensitive to the precise values of the electron current density, and may occur even if the ac voltage is less than 1% of the dc voltage. This instability is quite violent. In the low-frequency regime, breakdown of the flow may occur in less than one rf cycle of the ac voltage.

The unexpected results reported above were obtained from the electrostatic, one-dimensional code PDP1 [2]. The model is shown in Fig. 1, which shows a planar gap of gap separation D exposed to an external magnetic field $\hat{z}B$. The anode, located at $x = D$, is held at a voltage $V = V_0 + V_1 \sin(\omega t + \phi)$ with respect to the cathode, located at $x = 0$. Here, V_0 is the dc gap voltage and V_1 is the amplitude of the ac gap voltage of frequency ω and phase ϕ. We assume that all electrons are emitted from the cathode with the same initial energy $U_i = mu_0^2/2$ at the initial velocity $\hat{x}u_0$, and carrying an injected current of current density $\hat{x}J$.

When $V_1 = 0$, stable time-independent electron flows exist only if the injected current J is less than some critical value J_c [1,3–6]. If $J > J_c$, the electron flow quickly breaks into turbulence. This critical current J_c is shown in Fig. 2 for general values of B/B_H [5] where $B_H = \sqrt{(2mV_0/eD^2) + (mu_0/eD)^2}$ is the Hull cutoff magnetic field. When $B > B_H$ and $J < J_c$, all emitted electrons will return to cathode, after having reached the maximum height x_T (Fig. 1). Hereafter, we consider only the effect of a small ac gap voltage V_1 on such an initially time-independent, stable cycloidal flow ($B > B_H$, $J < J_c$). Specifically, two such initial states are studied: (A) $J = 0.75J_c$, $U_i = 0.5$ eV, as represented by the solid diamond in Fig. 2, and (B) $J = 0.25J_c$, $U_i = 5$ eV, as represented by the open diamond in Fig. 2. Note that case A represents a stable equilibrium flow with a high injection current and low injection velocity, whereas case B represents the opposite regime, viz., that of a stable equilibrium flow with a low injection current and high injection velocity.

The computer simulations for cases A and B were done using the electrostatic 1D code PDP1 [2] with the following parameters: $D = 2.16$ mm, $V_0 = 12$ kV, $B = 0.27$ T. There were 400 cells across the gap, and the cathode area was set at 31.22 cm^2.

Shown in Figs. 3 and 4 are the simulation results for case A of Fig. 2, when a small ac voltage $V_1 = 4$ V (0.033% of V_0) at the frequency $\omega/2\pi = 1$ GHz is imposed across the gap. Figure 3 shows the time history of the surface charge density on the cathode σ_c and the potential midway through the gap ϕ_{mid}, which is a vacuum potential. Three regions can be

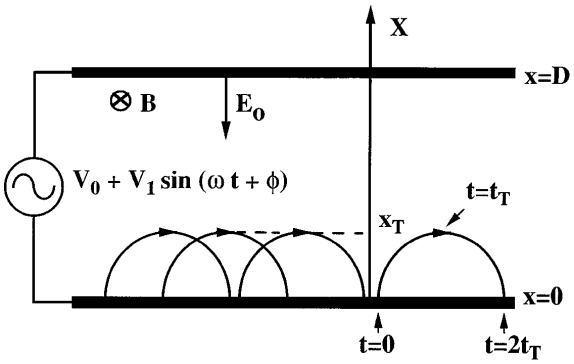

FIG. 1. The model. In the absence of the ac voltage V_1, an electron emitted at $x = 0$ at $t = 0$ reaches a maximum height $x = x_T$ at $t = t_T$, and returns to $x = 0$ at $t = 2t_T$.

 0031-9007/96/76(18)/3324(4)$10.00

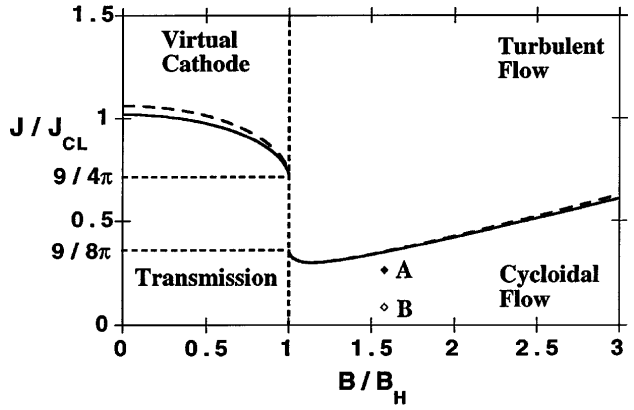

FIG. 2. The solid (dashed) curve shows the critical current density J_c, normalized to the Child-Langmuir value J_{CL}, when the injection energy is 0.5 eV (5 eV). The points A, B mark the cases simulated.

identified in Fig. 3: Region I shows a laminar state, region II shows the transition to turbulence, and region III shows the fully developed turbulent state. The phase space (v_x vs x) plot in the laminar region I is shown in Fig. 4(a); it exemplifies all of the electron orbits below the transition to turbulence, where all particles follow the same elliptical trajectory in the phase space. The phase space plot in the transition region II is shown in Fig. 4(b). There we see that the cycloidal orbit becomes perturbed as some electrons are slowed to $v_x = 0$ before reaching the cathode. These electrons will then spend a long time in front of the cathode surface, and their number increases as time goes on because electrons are continuously released from the cathode. This buildup of space charge retards the acceleration of the electrons especially in the immediate vicinity of the cathode and causes a contraction of the orbits in phase space. This contraction is especially apparent in the fully turbulent case [Fig. 4(c)] which shows the highly

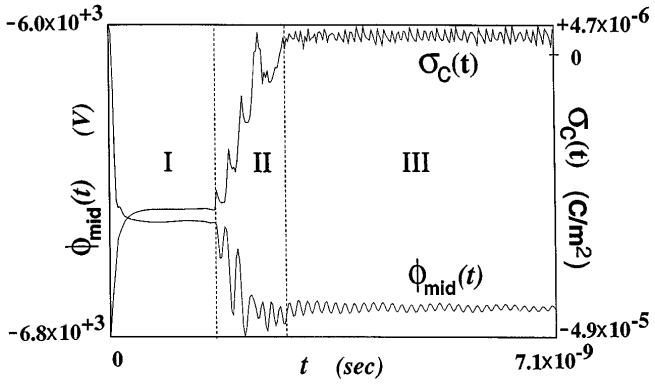

FIG. 3. Time history of the cathode surface charge density (σ_c) and of the electrostatic potential (ϕ_{mid}) midway inside the gap. Region I: laminar state; region II: transition to turbulence; region III: fully developed turbulent state.

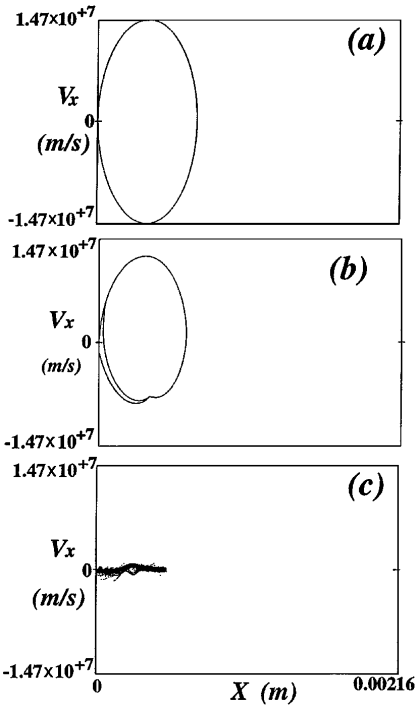

FIG. 4. Phase space plots for (a) laminar region I, (b) transition region II, and (c) fully developed turbulent region III.

randomized phase space typical of region III of Fig. 3, and this turbulent flow exhibits qualitative features of the classical Brillouin flow solution. The simulation at this late stage is practically indistinguishable from a case where the injected current density exceeded the critical current density ($J > J_c$ [5]). The potential at the midpoint oscillates at a frequency (Fig. 3) which is just below the cyclotron frequency (at 7.56 GHz), and well above the rf frequency (at 1 GHz) of the ac gap voltage. The cathode surface charge density σ_c oscillates about a positive value at a frequency which is not well resolved in the simulations. The fact that σ_c changes sign from region II to region III (Fig. 3) indicates the presence of a potential minimum. That is, a virtual cathode right in front of the cathode has been formed in region III. Note from Fig. 3 that turbulence is fully developed in less than three rf cycles.

The above simulation results for case A are qualitatively the same as case B whenever turbulence is triggered by the presence of a small ac gap voltage V_1. In fact, this transition to turbulence occurs over a wide range of V_1 and frequencies ω. In general, we find that at a given frequency ω there is a threshold rf voltage V_1 above which turbulence will develop and below which the flow remains laminar and stable. The simulation results are shown in Fig. 5 where the solid diamonds correspond to case A and the open diamonds correspond to case B. Each simulation point has a vertical bar 1 V in height. If the ac voltage V_1 lies below the bottom of the vertical bar, the flow remains

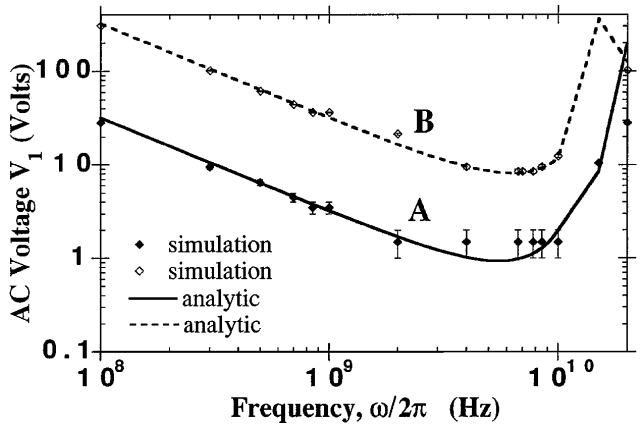

FIG. 5. Minimum ac gap voltage, V_1, as a function of frequency ω, for the onset of the modulational instability. Also shown is the analytic theory for both cases A and B.

laminar. If the ac voltage V_1 lies above the top of the vertical bar, the flow becomes turbulent. The simulation data shown in Fig. 5 suggest that when V_1 is sufficiently large the instability occurs over a finite (through large) band of frequencies.

The surprising result that a very small ac gap voltage, over a wide range of frequencies, leads to the breakdown of an initially stable flow is corroborated by the following simple analytic theory. We begin with the equation of motion of an electron, which reads

$$\ddot{x} + \Omega^2 x = -\frac{e}{m}\left[E_0(x) + E_1 \sin(\omega t + \phi) + E_s(x,t)\right], \tag{1}$$

where $\Omega = eB/m$ is the cyclotron frequency, $E_0(x)$ is the total dc electric field which includes both the vacuum field V_0/D *and* the dc space charge field, $E_1 = V_1/D$ is the ac vacuum field, and $E_s(x,t)$ is the additional space charge field in response to the ac gap voltage V_1. Long before the onset of turbulence, such as in region I of Fig. 3, one may argue that this additional space charge field E_s may be neglected, in which case the force law (1) yields the energy conservation relation

$$\frac{\dot{x}^2}{2} + \frac{\Omega^2 x^2}{2} + \frac{e}{m}\int_0^x dx\, E_0(x) = \frac{u_0^2}{2} - \frac{e}{m} E_1 \int_0^t dt\, \dot{x}(t) \sin(\omega t + \phi), \tag{2}$$

where we have used the initial condition that the electron is emitted from the cathode ($x = 0$) at time $t = 0$ with injection energy $U_i = mu_0^2/2$. It is clear that this electron will not return to the cathode ($x = 0$) if the right-hand side of Eq. (2) is less than zero, when evaluated at $t \approx 2t_T$ (Fig. 1). Thus, the condition for electrons to pile up in front of the cathode is approximately given by

$$\frac{U_i}{eV_1} < \frac{1}{D}\int_0^{t_T} dt\, \dot{x}(t)\left[\sin(\omega t + \phi) - \sin(\phi + 2\omega t_T - \omega t)\right] \tag{3}$$

for some ϕ. In writing (3), we have further assumed that the electron velocity $u(t) = \dot{x}(t)$ is subject only to the dc electric field $E_0(x)$ and magnetic field B, in which case $u(t) = -u(2t_T - t)$ for $t_T < t < 2t_T$ (Fig. 1).

Note that the inequality (3) is consistent with the simulation results that the modulational instability occurs only when V_1 exceeds some value, and only for a finite range of ω, as the right-hand side of (3) vanishes in the low-frequency limit $\omega \to 0$ and in the high-frequency limit $\omega \to \infty$.

The integral in Eq. (3) may readily be evaluated when we use the Llewellyn solution for $\dot{x}(t)$ [3,4],

$$\frac{\dot{x}(t)}{\Omega D} = 2\tilde{J} + (\tilde{u}_0 - 2\tilde{J})\cos(\Omega t) + \tilde{c}\sin(\Omega t), \tag{4}$$

where $\tilde{J} = eJ/m\varepsilon_0\Omega^3 D$, $\tilde{u}_0 = u_0/\Omega D$, and $\tilde{c}$ represents the initial acceleration of the electron; it is proportional to the dc electric field on the cathode surface [7]. The dimensionless quantities $\tilde{J}$, $\tilde{u}_0$, $\tilde{c}$, and $\tilde{t}_T \equiv \Omega t_T$ depend only on the dc condition. They are determined (numerically) from the Llewellyn solutions once D, B, V_0, J, and u_0 are specified [8]. Upon substituting (4) into (3), and maximizing the integral in (3) with respect to ϕ, we obtain the analytic results displayed in Fig. 5.

The stability boundaries shown in Fig. 5 have a simple analytic formula at low frequencies. We first substitute (4) into (3) and denote the right-hand member of (3) as $I(\omega)$. We next Taylor expand $I(\omega) \approx I(0) + \omega I'(0) = \omega I'(0)$ where the prime denotes differentiation with respect to ω [under the integral sign in (3)]. Equation (3), in the low-frequency limit ($\omega \ll \Omega$), then reads

$$\left(\frac{U_i}{eV_1}\right)\left(\frac{\Omega}{\omega}\right) < 2(\tilde{u}_0 + \tilde{c}\tilde{t}_T + \tilde{J}\tilde{t}_T^2), \tag{5}$$

upon setting $\phi = \pi$ and using $\dot{x}(t_T) = 0$. The right-hand member of the inequality (5) is independent of the ac gap voltage. It is of order unity typically [8].

Equation (5) gives the lower bound of the unstable frequency band once V_1 is given. On the other hand, for a given ω ($\omega \ll \Omega$), it yields the minimum value of V_1 for the excitation of the modulational instability. This minimum V_1 is proportional to $1/\omega$ for small ω according to Eq. (5), and is in excellent agreement with the simulation data displayed in Fig. 5 for $\omega/2\pi < 2$ GHz. This agreement confirms the piling up of electrons right in front of the cathode as the major cause of this modulational instability. Note that the low-frequency stability boundary, Eq. (5), is remarkably accurate for both the high injection

current case A ($J = 3J_c/4$) and the low injection current case B ($J = J_c/4$).

We have thus far not been able to provide a simple analytic estimate that reliably predicts the upper bound of the unstable frequency band. The following observations from our simulations also require further study: (a) the enhanced instability when the gap was resonantly driven at some value of ω a few percent less than Ω, and (b) a "superstable" point for case B at the frequency $\omega/2\pi \approx 15$ GHz.

The present study reveals, perhaps for the first time, a major difference in the multistream model (in which electrons are emitted from the cathode and return to the cathode in the equilibrium state as studied in this paper) and the single stream model (in which the electrons are injected externally in the form of a parallel, laminar flow) in a crossed-field gap [9]. The multistream electron flows are found to be intrinsically much more ready to develop into turbulence—the only requirement is an ac voltage across the gap approximately satisfying Eq. (5). This behavior is not expected in the single stream model. Although most crossed-field amplifiers and magnetrons are more closely approximated by the multistream model, at least during the initial stage of operation, this one-dimensional instability has not been suspected in the past because (1) the familiar diocotron instability requires a two-dimensional perturbation and (2) this modulational instability is closely related to the low energy electrons in the immediate vicinity of the cathode, and the microsheath right in front of the cathode is computationally expensive to resolve, especially in two-dimensional particle codes. It is also difficult to treat analytically. The present study reinforces the necessity to pay close attention to the low energy electrons near the cathode [6].

It remains to be seen whether the modulational instability reported here has any bearing on the difficult, unresolved problem of noise in crossed-field devices (including magnetron injection guns which are widely used in gyrotrons). This old problem of noise and unwanted frequencies in crossed-field devices continues to be of interest, one example being the interference with cellular communication by the magnetron in a microwave oven.

We are indebted to David Chernin, Spilios Riyopoulos, and Adam Drobot of SAIC, and to Ned Birdsall, John Verboncoeur, and V. P. Gopinath of UC Berkeley for many stimulating discussions. This work was supported by NRL, ONR, and AASERT.

[1] See, e.g., R. C. Davidson, *Physics of Nonneutral Plasmas* (Addison-Wesley, Redwood City, CA, 1990); J. D. Lawson, *Physics of Charged Particle Beams* (Oxford University Press, Oxford, 1988).

[2] PDP1 (Plasma Device Planar 1 Dimensional), © 1990–93 Regents of the University of California, Plasma Theory and Simulation Group, Berkeley, CA. Available from Software Distribution Office of the ILP, 205 Cory Hall, Berkeley, CA 94720, software@eecs.Berkeley. EDU. This is a one-dimensional electrostatic code that includes all three components of velocity.

[3] See, e.g., C. K. Birdsall and W. B. Bridges, *Electron Dynamics of Diode Regions* (Academic Press, New York, 1966), Chap. 5.

[4] Y. Y. Lau, P. J. Christenson, and David Chernin, Phys. Fluids B **5**, 4486 (1993).

[5] P. J. Christenson and Y. Y. Lau, Phys. Plasmas **1**, 3725 (1994).

[6] J. P. Verboncoeur and C. K. Birdsall, Phys. Plasmas **3**, 712 (1996).

[7] The factor of 2 in Eq. (4) arises because the space charge is due to both the departing electrons (from the cathode) and the returning electrons (to the cathode) when $B > B_H$. This factor of 2 also appears in Eqs. (1) and (2) of Ref. [5].

[8] For example, for cases A and B studied in this paper, respectively, the values of $(\tilde{J}, \tilde{u}_0, \tilde{t}_T, \tilde{c})$ are equal to (0.0148, 0.004088, 3.631, 0.1109) and (0.004969, 0.01293, 3.181, 0.1751). The right-hand member of Eq. (5) then equals 1.204 and 1.24, respectively, for cases A and B.

[9] See, e.g., E. Okress, *Crossed-Field Microwave Devices* (Academic, New York, 1961).